

Measurement of the top quark pair production cross section using the ATLAS detector at the LHC

Serban PROTOPOPESCU*

Brookhaven National Laboratory

E-mail: serban@bnl.gov

on behalf of the ATLAS Collaboration

Inclusive and differential cross sections of top quark pair production at $\sqrt{s} = 7$ TeV and $\sqrt{s} = 8$ TeV measured with the ATLAS detector at the LHC are presented. All measurements are in good agreement with Standard Model predictions.

*XXIII International Workshop on Deep-Inelastic Scattering
27 April - May 1 2015
Dallas, Texas*

*Speaker.

1. Introduction

According to the Standard Model (SM) over 99% of the top quark decays are to $W + b$ -quark. The W decays generate the different $t\bar{t}$ channels. Measurements in individual channels really are measurements of $\sigma_{t\bar{t}} \cdot BR_1 \cdot BR_2$ where BR_1 and BR_2 are the branching ratio of t and \bar{t} . To obtain the inclusive $\sigma_{t\bar{t}}$ all measurements assume the top quark branching ratios into final states with leptons and/or jets are determined by the branching ratios for the W decay. Inclusive $\sigma_{t\bar{t}}$ measured with different final states inconsistent with each other or with the SM would be evidence for new physics. Non-SM processes such as $t \rightarrow H^+ b$, $t \rightarrow \tilde{t} + X$ or $\tilde{t}\tilde{t}^*$, where \tilde{t} stands for the supersymmetric partner of the top quark, can produce more events than expected from the SM in some or all channels. The cross sections for top-antitop pair production measured with the ATLAS detector [1] in pp collisions at $\sqrt{s} = 7$ TeV and $\sqrt{s} = 8$ TeV using three final states are reported:

ℓ +jets: exactly one isolated e ($p_T^e > 25$ GeV) or exactly one isolated μ ($p_T^\mu > 20$) GeV, ≥ 3 jets (anti- k_r algorithm $R = 0.4$, $p_T > 25$ GeV) and at least one tagged as a b -jet (b -tag). An isolated electrons must pass a calorimeter based E_T isolation requirements within a cone $\Delta R = 0.2$ and a track based p_T isolation requirements within a cone $\Delta R = 0.3$. The distance ΔR in η - ϕ space is defined as $\Delta R = \sqrt{(\Delta\phi)^2 + (\Delta\eta)^2}$. An isolated μ must pass a calorimeter based E_T isolation requirement within a cone $\Delta R = 0.2$. Additional requirements (not used for the other channels) were $E_T^{miss} > 30$ GeV, $m_T(W) > 30$ GeV for e +jets, and $E_T^{miss} > 20$ GeV, $m_T(W) + E_T^{miss} > 60$ GeV for μ +jets, where $m_T(W) = \sqrt{(E_T^\ell + E_T^{miss})^2 - (p_x^\ell + E_x^{miss})^2 - (p_y^\ell + E_y^{miss})^2}$. For the 8 TeV sample the lepton p_T thresholds were raised to 40 GeV.

$\ell\tau$ +jets: same e and μ requirements as for ℓ +jets, one τ lepton decaying to hadrons (τ_{had} , $p_T^\tau > 20$ GeV), and ≥ 2 jets with $p_{T>25}$ GeV. The τ candidate was required to have at least one and no more than three associated tracks.

$e\mu+b$ -jet: same e and μ requirements, exactly one isolated e and exactly one isolated μ , and ≥ 1 b -jet (jets containing b hadrons).

The differential cross section measurements were done using only the ℓ +jets final state.

2. Inclusive $\sigma_{t\bar{t}}$ Measurements

The inclusive $t\bar{t}$ production cross sections have been measured with ℓ +jets events at $\sqrt{s} = 7(8)$ TeV using a data sample of $\int L dt = 4.66(20.3)$ fb $^{-1}$ [2, 3]. The b -tag methods used in the 7 TeV sample and 8 TeV sample were different. The b -tag in the 7 TeV sample was a soft- μ with $p_T^\mu > 4$ GeV within a cone $R=0.5$ of the jet; in all other measurements the b -tag was based on a multivariate discriminant.

The measurements with 7 TeV and 8 TeV data were both based on a fit to a likelihood discriminant with Monte Carlo (MC) signal and background templates. Data are compared to MC based predictions for the signal and combined backgrounds. For 7 (8) TeV analysis the signal and the single top background were derived from MC $t\bar{t}$ simulation using the MC@NLO [5] generator (POWHEG [6]) interfaced to HERWIG [7] and JIMMY [8] (PYTHIA [9]) for showering, hadronization and the underlying-event. The W +jets and Z +jets background were simulated using ALPGEN [11] interfaced to HERWIG. The W +jets normalization was obtained using data-driven techniques exploiting the fact that more W^+ than W^- are produced. The multi-jet background was

derived from data. The numbers of events in the 7 TeV sample were 9165 e +jets and 14894 μ +jets with a one-to-one signal to background ratio($S/B=1/1$). The number of events in the 8 TeV sample were 176286 e +jets and 220369 μ +jets with $S/B=2/1$. Figure 1 gives m_T for the 7 and 8 TeV μ +jets events and shows that the data and the model predictions are in good agreement. The distributions from e +jets events (not shown) are in similar good agreement. The measured inclusive cross sections combining the e +jets and μ +jets channels were:

$$\sigma_{t\bar{t}} = 165 \pm 2(\text{stat.}) \pm 17(\text{syst.}) \pm 3(\text{lumi.}) \text{ pb at 7 TeV}$$

$$\sigma_{t\bar{t}} = 260 \pm 1(\text{stat.})_{-23}^{+22}(\text{syst.}) \pm 8(\text{lumi.}) \pm 4(\text{b.e.u.}) \text{ pb at 8 TeV}$$

where $b.e.u.$ stands for beam energy uncertainty. The dominant systematic uncertainties at 7 TeV are the background (7.3%) and signal (5.2%) models, while at 8 TeV it is the signal model (7.6%).

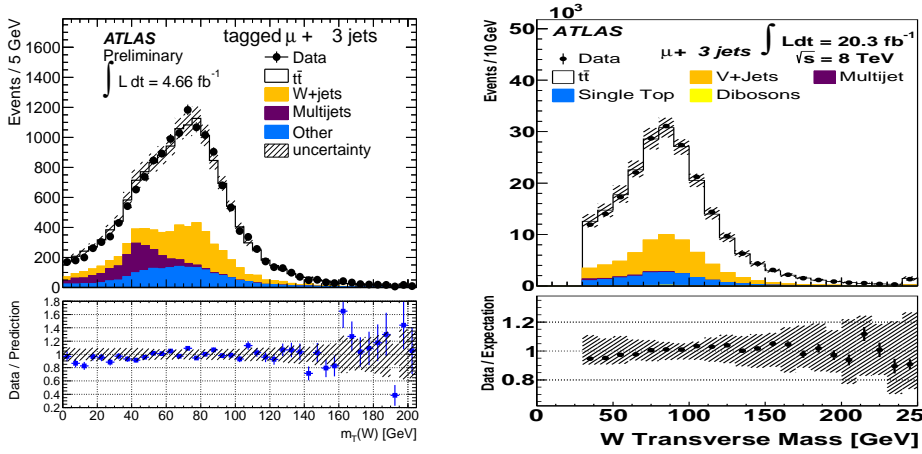


Figure 1: Transverse mass of μ +jets events at 7 TeV [2] and at 8 TeV [4].

The inclusive $t\bar{t}$ production cross sections has been measured with $\ell\tau$ +jets events at $\sqrt{s} = 7$ TeV using a data sample of $\int L dt = 2.05 \text{ fb}^{-1}$ [10]. This final state is of particular interest because a number of non-SM processes predict final states favoring decays to τ leptons such as $t \rightarrow H^+ (\rightarrow \tau\nu) + b$ and $\tilde{t} \rightarrow b\nu_t \tilde{\tau} (\rightarrow \tau + \text{gravitino})$. The data sample selected for the cross section measurement with $\ell\tau$ +jets events is split into two subsamples: events with ℓ and τ candidates of opposite-sign charge (OS) and events with ℓ and τ candidates of same-sign charge (SS). In turn the subsamples are split into a sample with no b -tags and a sample with at least one b -tag. A Boosted Decision Tree discriminant BDT_j (BDT_e), was used to separate jets (electrons) misidentified as τ leptons from τ leptons. The electron background was removed by requiring a minimum value for BDT_e . The cross section measurement was based on fits with background templates and signal templates to derived BDT_j distributions obtained by subtracting SS distributions from OS distributions (OS–SS). BDT_j OS–SS distributions can only have contributions from jets originating from leading quarks misidentified as τ 's since jets originating from gluons cannot be charge correlated. The signal template was based on MC simulation using the same generators as for the

ℓ +jets channel at 7 TeV. The data-driven background template was derived from the sample with no b -tags. The fits were done separately to τ candidates with only one associated charged track and those with more than one, because the BDT_j distributions are very different as shown in Fig. 2. The measured inclusive cross section was:

$$\sigma_{t\bar{t}} = 186 \pm 13(\text{stat.}) \pm 20(\text{syst.}) \pm 7(\text{lumi.}) \text{ pb}$$

The dominant systematic uncertainty in this measurement was the one associated with b -tagging (9%).

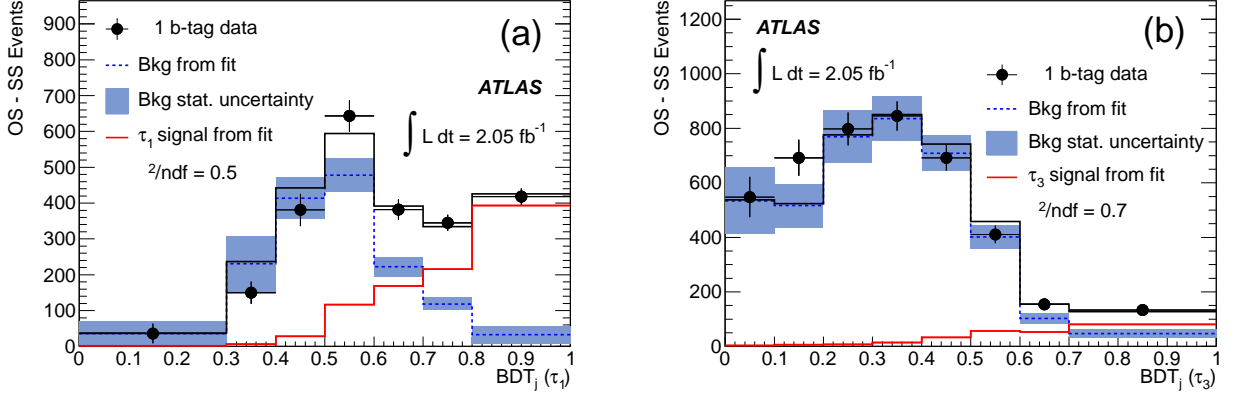


Figure 2: OS–SS BDT_j distributions [10]: (a) 1-prong τ candidates, (b) multiprong τ candidates.

The $e\mu+b$ -jet channel gave the most precise measurement of the inclusive $\sigma_{t\bar{t}}$ at $\sqrt{s} = 7$ TeV and at $\sqrt{s} = 8$ TeV using the full data samples, $\int L dt = 4.6 \text{ fb}^{-1}$ and $\int L dt = 20.3 \text{ fb}^{-1}$, respectively [12]. The analysis methods consisted of counting events with exactly one (N_1) and exactly two (N_2) b -tags expressed as

$$N_1 = L\sigma_{t\bar{t}}\epsilon_{e\mu}2\epsilon_b(1 - C_b\epsilon_b) + N_1^{bkg}, \quad N_2 = L\sigma_{t\bar{t}}\epsilon_{e\mu}\epsilon_b^2 C_b\epsilon_b^2 + N_2^{bkg}$$

where $\epsilon_{e\mu}$ is the $e\mu$ efficiency, ϵ_b is the b -tag efficiency and C_b is a b -tagging correlation coefficient close to unity. Figure 3 shows the distributions for signal and background of the number of b -tags. The number of signal (background) N_1 and N_2 events at 7 TeV are 3527(400) and 2073(70) respectively, and at 8 TeV 21666(2590) and 11739(460) respectively. The backgrounds were predicted from MC simulation using the same generators listed earlier.

The measured cross sections were

$$\sigma_{t\bar{t}} = 182.9 \pm 3.1(\text{stat}) \pm 4.2(\text{syst}) \pm 3.6(\text{lumi}) \pm 3.3(\text{b.e.u.}) \text{ pb at 7 TeV}$$

$$\sigma_{t\bar{t}} = 242.4 \pm 1.7(\text{stat}) \pm 5.5(\text{syst}) \pm 7.5(\text{lumi}) \pm 4.2(\text{b.e.u.}) \text{ pb at 8 TeV}$$

The uncertainties in the luminosity and the beam energy significantly limit the precision of these measurements. Combining these measurements one can extract the mass of the top quark at the pole (used in theoretical calculations) with good precision: $172.9_{-2.6}^{+2.5}$ GeV. One can also exclude with 95% confidence level the pair-production of supersymmetric top squarks (\tilde{t}) with masses between the top quark mass and 177 GeV if \tilde{t} decays predominantly to a right-handed top quark and a neutralino with mass = 1 GeV.

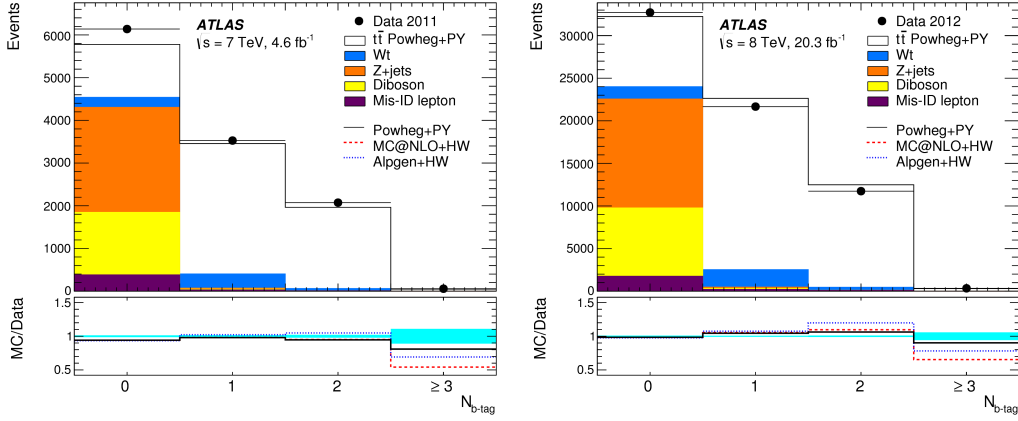


Figure 3: Number of b -tags in events at 7 TeV and at 8 TeV [12].

3. Differential $\sigma_{t\bar{t}}$ Measurements

Differential cross sections are sensitive to the parton density functions (DPF) and are useful for tuning and constraining MC event generators. The 7 TeV data samples and backgrounds estimators used were the same as for the ℓ +jets inclusive $\sigma_{t\bar{t}}$ measurement. The $t\bar{t}$ kinematics was reconstructed by maximizing a kinematic likelihood that was the product of the W boson and top quark Breit-Wigner distributions, and transfer functions representing the experimental resolutions in terms of the probability that the observed energy at reconstruction level is produced by a parton-level object with a certain energy [13]. The resulting differential cross sections as function of the top quark transverse momentum (p_T^t) and the transverse momentum ($p_T^{t\bar{t}}$), mass ($m_{t\bar{t}}$), and rapidity ($y_{t\bar{t}}$) of the $t\bar{t}$ system (after background subtraction) were compared to those predicted using three different MC generators: MC@NLO, ALPGEN and POWHEG. The results are shown in Fig. 4.

POWHEG+PYTHIA provides the best description of $d\sigma_{t\bar{t}}/dp_T^t$ and $d\sigma_{t\bar{t}}/dp_T^{t\bar{t}}$ while ALPGEN+HERWIG is closer to $d\sigma_{t\bar{t}}/dm_{t\bar{t}}$ and $d\sigma_{t\bar{t}}/d|y_{t\bar{t}}|$. Systematic uncertainties dominate, ranging from 4% at low p_T to 16% at high p_T . For $d\sigma_{t\bar{t}}/dp_T^t$ and $d\sigma_{t\bar{t}}/dm_{t\bar{t}}$ the largest uncertainties are from jet energy scale, signal generator choice and b -tagging efficiency. For $d\sigma_{t\bar{t}}/dp_T^{t\bar{t}}$ the dominant uncertainty comes from initial and final state radiation while for $d\sigma_{t\bar{t}}/d|y_{t\bar{t}}|$ it is the signal generator choice and jet fragmentation.

The dependence of the measured differential cross-sections on theoretical models can be greatly reduced by presenting them in terms of kinematic variables of a top-quark proxy referred to as a pseudo-top-quark (\hat{t}), which is defined by either reconstructed objects in the detector or stable particles in an analogous way. The cross section can be measured for both hadronic \hat{t} (\hat{t}_h) and leptonic \hat{t} (\hat{t}_l) depending on the W boson decay. For these measurements the ℓ +jets sample was required to have at least two b -tagged jets [14]. Figure 5 show the results for $d\sigma_{\hat{t}\bar{\hat{t}}}/dp_T^{\hat{t}}$, $d\sigma_{\hat{t}\bar{\hat{t}}}/dp_T^{\hat{t}\bar{\hat{t}}}$, $d\sigma_{\hat{t}\bar{\hat{t}}}/m_{\hat{t}\bar{\hat{t}}}$. The $d\sigma_{\hat{t}\bar{\hat{t}}}/dp_T^{\hat{t}}$ is in good agreement with $d\sigma_{\hat{t}\bar{\hat{t}}}/dp_T^{\hat{t}_h}$, shown in Fig. 6. MC events generated with POWHEG+PYTHIA using HERA15NLO PDF [15] agree well and better than all others with the data.

At high p_T^t , jets originating from top quarks will tend to be collimated and merge (boosted-top quarks). To extend the measurements to $p_T^t > 300$ GeV, event selection needs to be modified. The

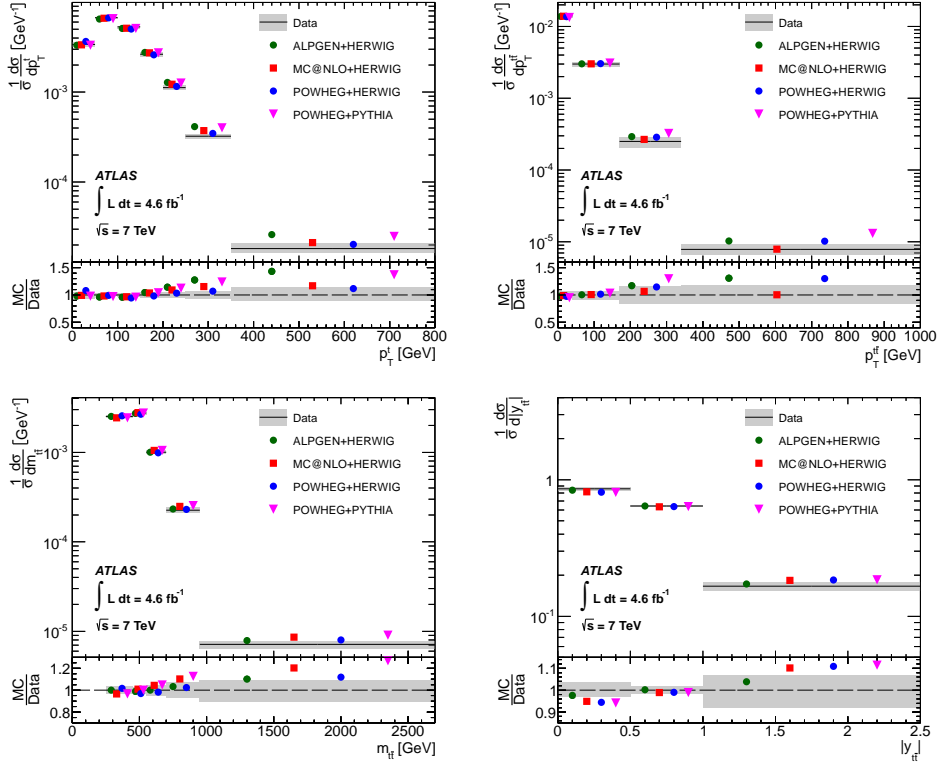


Figure 4: The differential cross section for $t\bar{t}$ production as function of p_T^t , $p_T^{\bar{t}}$, $m_{t\bar{t}}$ and $|y_{t\bar{t}}|$ [13].

jet requirements for the selection of ℓ +jets events at 8 TeV were at least one $R=0.4$ jet with $p_T > 25$ GeV, $|\eta| < 2.5$, exactly one $R=1.0$ jet with $p_T > 300$ GeV, $|\eta| < 2.0$ and at least one $R=0.4$ b -jet with ΔR between lepton and b -jet < 1.5 or ΔR between $R=1.0$ jet and b -jet < 1.0 [16]. Using events with boosted-top quarks extends the range of $d\sigma_{t\bar{t}}/dp_T^{\hat{t}}$ to 1.0 TeV as shown in Fig. 6.

4. Conclusion

The inclusive $\sigma_{t\bar{t}}$ measured with the ATLAS detector in $\sqrt{s} = 7$ TeV pp collisions with ℓ +jets, $\ell\tau$ +jets and $e\mu$ + b -jet events are in very good agreement with each other and so are those measured in $\sqrt{s} = 8$ TeV pp collisions with ℓ +jets and $e\mu$ + b -jet events. The measurements using $e\mu$ + b -jet are the most precise, 183 ± 7 pb at 7 TeV and 242 ± 10 pb at 8 TeV. These are in excellent agreement with SM next-to-next-to-leading order (NNLO) plus next-to-next-to-leading-logarithm (NNL) calculations, 177 ± 10 pb and 253 ± 14 pb [17]. Differential $\sigma_{t\bar{t}}$ has been measured with ℓ +jets events in $\sqrt{s} = 7$ TeV pp collisions and compared to predictions from a number of MC event generators. POWHEG reproduces the distributions better than ALPGEN or MC@NLO. A boosted-top algorithm extends the measurement of $d\sigma_{t\bar{t}}/dp_T^{\hat{t}}$ at 8 TeV to $p_T^{\hat{t}} > 1.0$ TeV. For $p_T^{\hat{t}} > 300$ GeV all generators predict harder $d\sigma_{t\bar{t}}/dp_T^{\hat{t}}$ than observed.

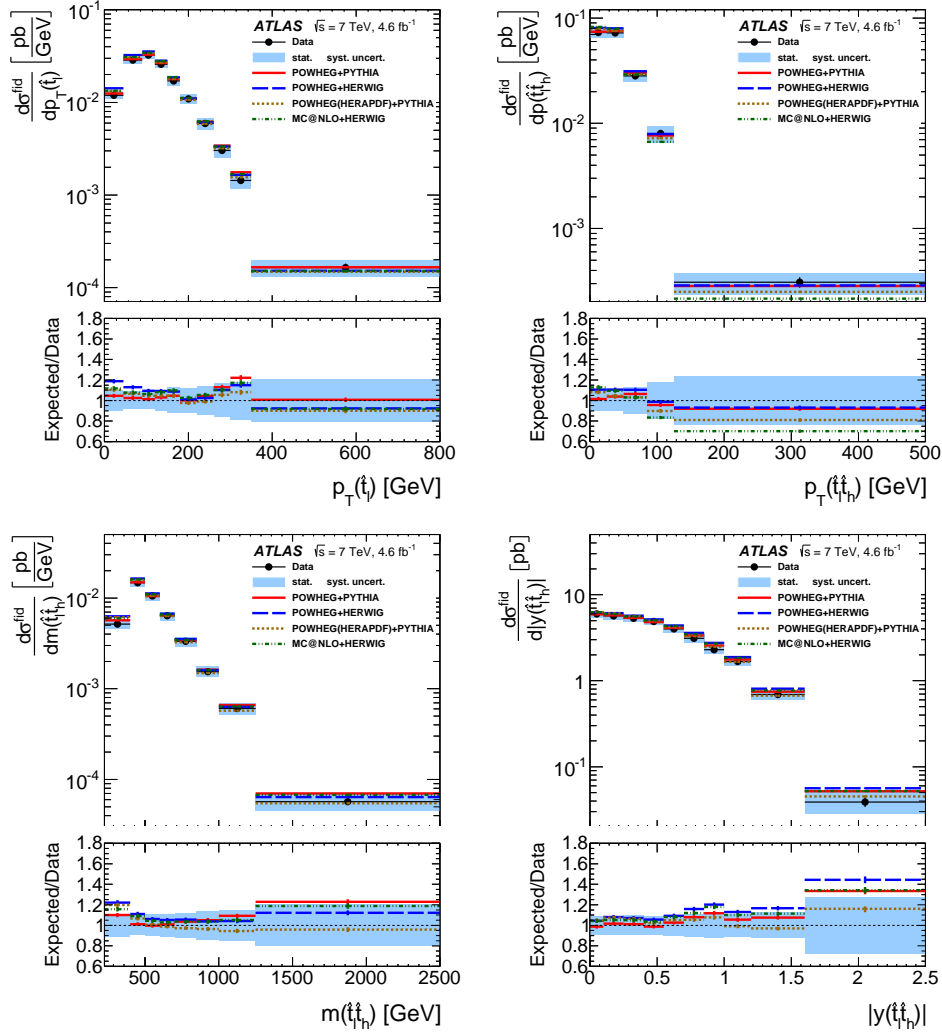


Figure 5: The fiducial differential $t\bar{t}$ cross section as function of the leptonic pseudo-top-quark variables p_T^i , $p_T^{\bar{i}}$, $m_{t\bar{t}}$ and $|y_{t\bar{t}}|$ [14].

References

- [1] ATLAS Collaboration, 2008 JINST 3 S08004.
- [2] ATLAS Collaboration, ATLAS-CONF-2012-131, <http://cds.cern.ch/record/1478370>.
- [3] ATLAS Collaboration, Phys. Rev. D **91** 2015 112013 .
- [4] ATLAS Collaboration, <http://atlas.web.cern.ch/Atlas/GROUPS/PHYSICS/PAPERS/TOPQ-2013-06/>.
- [5] S. Frixione, E. Laenen and B. R. Webber, JHEP **03** (2006) 092.
- [6] S. Alioli, P. Nason, C. Oleari and E. Re, JHEP **06** (2010) 043.
- [7] G. Corcella et al., JHEP **01** (2001) 010.
- [8] J. M. Butterworth et al., Zeit. für Phys. **C72** (1996) 637.

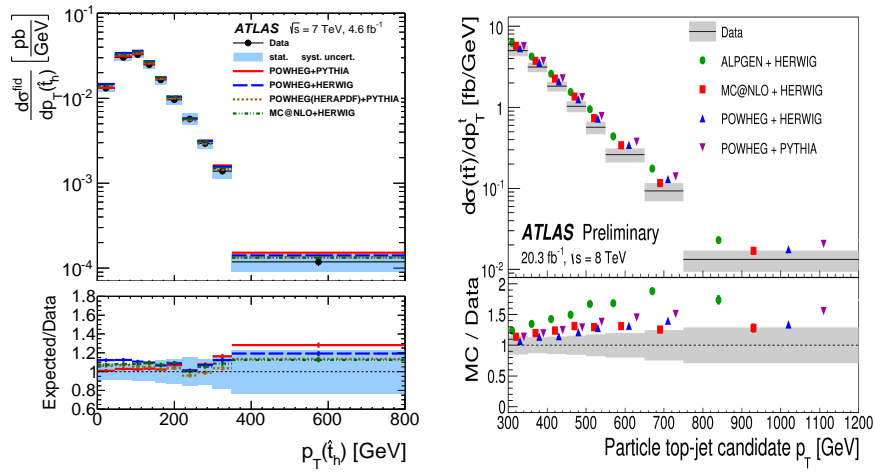


Figure 6: $d\sigma_{t\bar{t}}/dp_T^{\hat{t}_h}$ for nonboosted-top quarks at 7 TeV [14] and boosted-top quarks at 8 TeV [16].

- [9] T. Sjostrand et al., JHEP **05** (2006) 026.
- [10] ATLAS Collaboration, Phys. Lett. B **717** (2012) 89.
- [11] M. L. Mangano et al., JHEP **07** (2003) 001.
- [12] ATLAS Collaboration, Eur. Phys. J **74** (2014) 3109.
- [13] ATLAS Collaboration, Phys. Rev. D **90** (2014) 072004.
- [14] ATLAS Collaboration, JHEP **06** (2015) 100.
- [15] H1 and Zeus Collaborations, JHEP **01** (2010) 109.
- [16] ATLAS Collaboration, ATLAS-CONF-2014-057, <http://cds.cern.ch/record/1951328>.
- [17] M. Czakon and A. Mitov, Comp. Phys. Comm. **182** (2014) 2930.